

# Observed Directional Wave Spectra During a Frontal Passage

Neil E. Van de Voorde<sup>†</sup> and Scott P. Dinnel<sup>‡</sup>

<sup>†</sup>National Data Buoy Center  
Building 1100  
Stennis Space Center, MS  
39529, U.S.A.

<sup>‡</sup>Center for Marine Science  
University of Southern  
Mississippi  
Stennis Space Center, MS  
39529, U.S.A.

## ABSTRACT

VAN DE VOORDE N.E. and DINNEL, S.P., 1998. Observed directional wave spectra during a frontal passage. *Journal of Coastal Research*, 14(1), 337-346. Royal Palm Beach (Florida), ISSN 0749-0208.



This paper qualitatively discusses the changes in the directional wave field as the result of an atmospheric cold front passage. The directional wave data were measured using a 3-m discus buoy in the north-eastern Gulf of Mexico using a Longuet-Higgins technique with 46 frequency bands (0.0325 to 0.485 Hz).

Changes in the directional wave spectra were examined during a 4-day period that included a major wind shift under both quasi-steady and nonsteady wind fields. A procedure of combining the wave-energy into four directional quadrants, in lieu of individual mean directions, was examined as an analytical time-series technique for directional wave spectra. The lag time between a wind speed increase and a corresponding increase in wave-energy was shown to be a function of the existing sea state with shorter lag times for a higher sea condition. A numerical model analysis of VAN VLEDDER and HOLTHULSEN (1988) indicated that after a major wind shift the wave-energy would not only move to lower frequencies, but would also rotate to realign with the direction of the older wind field. The conclusions of VAN VLEDDER and HOLTHULSEN (1988) were supported by direct observations of pre- and post-frontal wave fields. Hourly, polar contoured, directional wave spectra plots show a narrow frequency band energy bridge between the two wave fields. The development of an energy bridge is shown to correspond to a change in the decay rate of the old wave field.

**ADDITIONAL INDEX WORDS:** *Directional waves, wave energy, wave-energy lag time, wave field data, northeastern Gulf of Mexico, National Data Buoy Center (NOAA), nonlinear wave process, and cold-front.*

## INTRODUCTION

Wave field response to changes in the wind field is of great interest to both the oceanographic and engineering communities. An understanding of the energy flux during dynamic wind conditions is critical to understanding the nonlinear processes occurring during wave field evolution. One such dynamic wind condition, where winds undergo both magnitude and directional changes, occurs during passage of atmospheric fronts and results in the decay of one wave field and the generation of another. There have only been few direct observations of wave field response to rapid wind changes using field data (ALLENDER *et al.*, 1983; YOUNG *et al.*, 1987; MASSON, 1990; and JACKSON and JENSEN, 1995). Much of the current effort has focused on the use of simulation models, such as the EXACT-NL (YOUNG *et al.*, 1987) and the 3G-WAM models (VAN VLEDDER and HOLTHULSEN, 1993). These models allow relatively simple changes in environmental inputs, *i.e.* a slowly varying wind speed and/or direction. However, frontal passages do not exhibit monotonically changing wind fields; their time histories are typically com-

plex. Changes in wind direction do not back or veer smoothly nor simply change in magnitude from pre-frontal to post-frontal conditions. Frontal passages, especially cold fronts, move rapidly and typically have unsteady winds (HSU, 1988). Thus, if models are to be used to simulate real wave data, the inputs of wind speed and direction should be updated continuously. A continuously updated wind field may be impractical for many applications; thus, a better understanding of the physics between the wind and wave fields during dynamic events may lead to the improvement of these models. JACKSON and JENSEN (1995) specifically discuss the need to improve the wave models' implementation of the physics of nonlinear wave-wave interaction. The observational nature of our paper is meant to point out certain aspects of the wind-wave dynamics occurring during rapid wind shifts.

Historic *in situ* buoy measurements have been insufficient in detail in the higher-frequency bands to examine the short-term effects of frontal passages. What has been done in the past using large 10- or 12-m buoys with a substantial battery array can be done today with a solar-powered 3-m or smaller discus buoy. The reduction in size and mass of the buoy has resulted in improved surface-following characteristics, especially with respect to the higher-frequency components. This has allowed the energy in the higher frequencies to be better measured, thus expanding the data set into that part

96004 received 9 February 1996; accepted in revision 5 January 1997.

<sup>†</sup> Current address: Commander, Eighth Coast Guard District, 501 Magazine St. New Orleans, LA 70130, USA.

<sup>‡</sup> Current address: Coastal Studies Institute, Louisiana State University, Baton Rouge, LA 70803, USA.

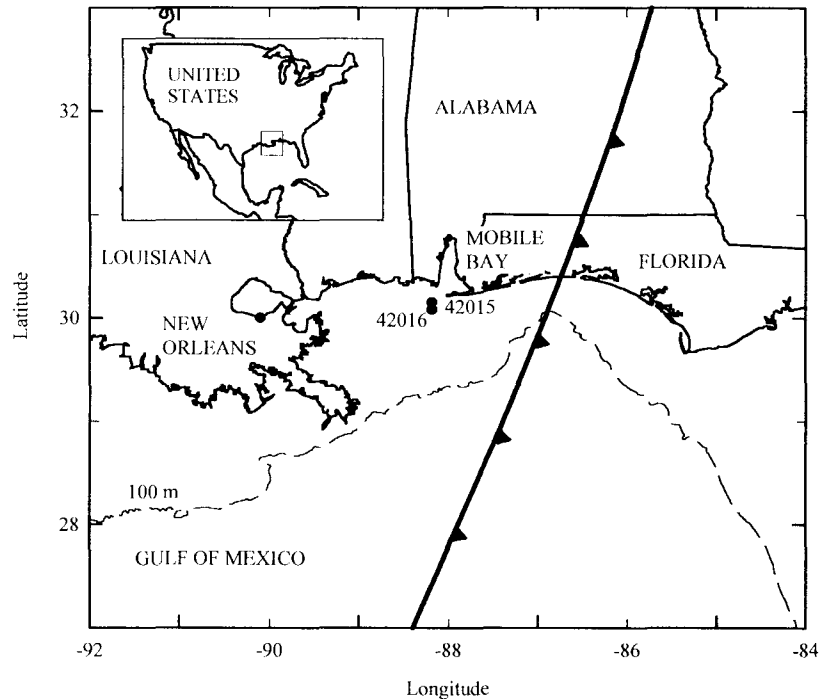


Figure 1. Location of NOAA Buoy 42015 and 42016 in coastal NE Gulf of Mexico. The location of the cold front is based upon an National Meteorological Center Surface Analysis chart for March 10, 1994, 0300 UTC.

of the wave spectra that is needed for an analysis of directional wave spectra changes during a major wind shift.

A National Data Buoy Center (NDBC) 3-meter disc buoy, located at National Oceanic and Atmospheric Administration's (NOAA) Buoy Station 42016 (30.08°N; 88.18°W) in the northeast Gulf of Mexico, was established in December 1993 and remained on station until early 1995 (Figure 1). The station was in approximately 30 m of water, and the distance offshore was approximately 37 km (~20 nm) from the entrance to Mobile Bay, Alabama. This station provided the platform from which all observations were made.

#### DATA MEASUREMENTS AND ANALYSIS

Directional wave spectra were computed from the nondirectional energy spectra, represented by a sea-surface elevation auto-spectrum,  $C11(f)$ , (*i.e.* the spectral variance based on the linear theory spectral components of the wave height for individual frequency bins) and a corresponding time series of the direction of the sea-surface tilt. The sea-surface tilt was used to develop a parametric directional spreading function,  $D(f, \theta)$ , where  $f$  was the center of a frequency band, and  $\theta$  was a mean direction.

A standard cosine-2s parametric model (LONGUET-HIGGINS *et al.*, 1963) was used as the basis for  $D(f, \theta)$  and produced an estimate of the angular width of the energy within each frequency band. The cosine-2s model allowed only one principle direction per frequency band of wave-energy. The drawback was that any energy present from two distinct directions, contained within the same frequency band, would

be assigned to a third direction between the two actual directions (YOUNG, 1994). This would have been a problem if the wave fields had overlapped in  $f$ -space; but we were fortunate that this was not the case. In further support of using the cosine-2s energy distribution model, QUANDUO and KOMEN (1993) analyzed the correlation between the cosine-2s model and the output from 3G-WAM during a 60° wind-shift episode. QUANDUO and KOMEN (1993) found that the high correlation, 0.97, between the parametric cosine-2s model and the 3G-WAM model output was due to the fact the most of the energy was located in the mean wave-direction. Therefore, in our case, since the "old" wave-energy (pre-wind shift) and the "new" wave-energy (post-wind shift) were widely separated in both  $f$ -space and  $\theta$ -space, the authors felt justified in the use of the cosine-2s energy distribution model.

NDBC's Waves Processing Module (WPM) measures vertical acceleration, which is converted using linear wave theory to  $C11(f)$ , north-south, and east-west buoy tilts. Orthogonal buoy tilts are converted to water-surface slopes. Estimates of the directional wave spectra can be obtained using the method of LONGUET-HIGGINS *et al.* (1963). A complete description of the basic theory of LONGUET-HIGGINS *et al.* (1963), and how it is currently implemented on buoys, can be found in STEELE *et al.* (1992, 1985) or TUCKER (1989).

NDBC's estimations of wave parameters ( $C11(f)$  and parameters for estimating  $D(f, \theta)$ ) are based upon 4096 data points sampled over 40-minutes, processed, and transmitted to shore hourly. The full data set (4,096 data points) are used to estimate the lower thirteen frequencies at a resolution of

0.005 Hz between 0.0325 Hz and 0.0925 Hz. The next 26 frequency estimations are based upon 2,048 data points from the last twenty minutes of the 40 minute data record. The resolution of this midrange is 0.01 Hz for bands between 0.1000 Hz and 0.3500 Hz. The final ten minutes of the 40 minute data record (1,024 data points) are used to estimate the high frequency tail using seven frequencies with a resolution of 0.02 Hz for a band between 0.3650 Hz and 0.4850 Hz. Spectra and cross-spectra are calculated without use of a leakage reduction window (EARLE, 1994). The hull is assumed to be a surface follower. It is also assumed that the hull-mooring response induces a frequency-dependent non-unity response amplitude operator (RAO) and nonzero phase shift angles. A detailed discussion of how the RAO and phase shifts are adjusted can be found in STEELE *et al.* (1992).

In analyzing the hourly directional wave data, we determined that the standard approach of using a time series for several specific narrow frequency bands (ALLENDER *et al.*, 1983; WANG *et al.*, 1989; MASSON, 1990) did not provide a clear picture of how the wave-energy changed during the major wind shift. Higher frequency bands reacted fairly quickly to changes in the wind field. Narrow frequency bands of wave-energy typically showed a large amount of variability. The combination of these two traits could mask correlations or general trends in the data record. We broadened the frequency bands into larger bins, which increased the statistical significance of each estimate and provided a filtering process via averaging. The trends in energy change in each frequency band were more readily discernable with the broader bands.

Five frequency bins were established to map out the flux of energy in time: 0.0325 to 0.08 Hz, 0.08 to 0.18 Hz, 0.18 to 0.22 Hz, 0.22 to 0.30 Hz, and 0.30 to 0.485 Hz. The bin boundaries were qualitatively selected by examining various one-dimensional spectra of C11(f) for changes during the frontal passage. Bin 1 (0.0325 to 0.08 Hz) was chosen to describe the swell wave field, which was not locally generated and was not considered in our analysis.

Bin 4 (0.22 to 0.30 Hz) was selected for use as a wind-energy tracer bin. Several authors (GUNTHER *et al.*, 1981; ALLENDER *et al.*, 1983; YOUNG *et al.*, 1987; ACINAS, 1988; MASSON, 1990) have indicated that higher-frequency components of the wave field respond quicker to changes in the wind field than the lower frequency wave components. Additionally, there was very little energy present in the upper "tail" of the wave spectra (*i.e.*, bin 5). The energy contained in bin 4 had a higher degree of what can be described as wave-energy momentum. That is, the energy was sufficient to resist responding to the higher frequency variability of the wind field, while responding to the wind field's general trends. Maintaining bin 5 separate from bin 4 provided the information on the initial transfer of energy from the wind field into the wave field. Energy in bin 4 was the result of energy shifting down from higher frequencies (bin 5) and possibly up from lower frequencies (bin 3). This type of energy transfer has been proposed by YOUNG *et al.* (1987). Bin 4 then contained information from the higher frequency, younger wave components, as well as mid-range frequency, possibly older, wave components.

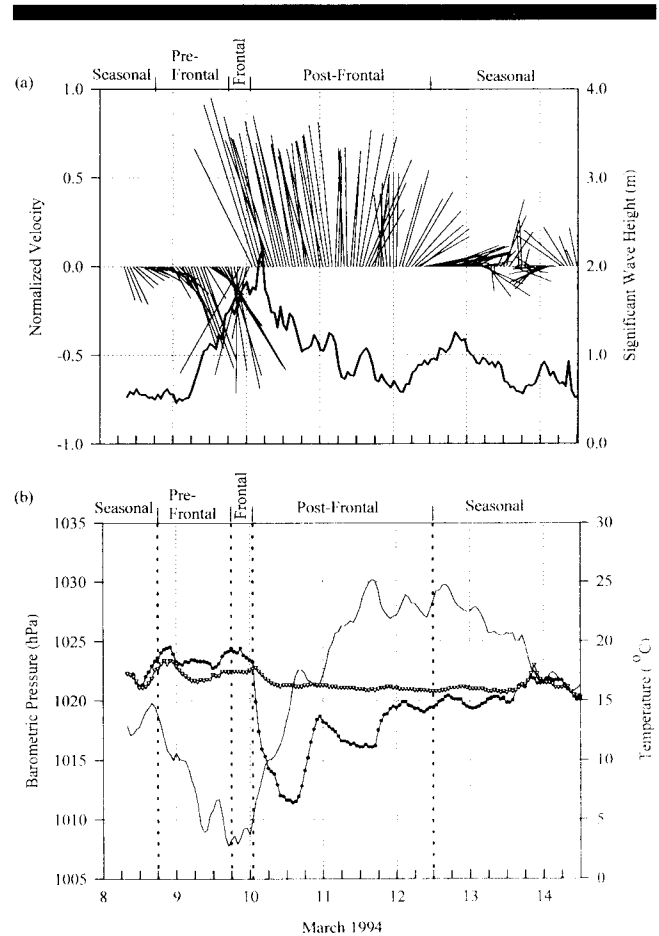


Figure 2. Data from NOAA Buoy station 42016. (a) The normalized wind velocity record covering the period of the frontal passage. The hourly wind velocity values have been normalized to the maximum wind speed of 13.1 m/sec. This maximum occurred at March 10, 1994, 0400 UTC, from a direction of 330° T. The height of the wind sensor was 5 m above the mean water line of the 3-m discus buoy. Significant wave height ( $H_s$ ) is shown for comparison with the wind record. (b) Hourly values for the air temperature (●), sea-surface temperature (○), and barometric pressure (—).

Reasoning similar to that used in the formation of the bins was used to initially establish four directional quadrants to partition the wave-energy. The mean direction for each of the bins was expected to display an unnecessary amount of variability for our analysis. Also, a simple analysis of old versus new wave-energy hid some of the information on how the energy was transferred between the old to the new wave fields. Thus, the four quadrant system was employed to allow the directionality of the energy field to be better followed in time.

## PHYSICAL SETTING

A single Continental-Polar cold front passage occurring in early March 1994, was selected for analysis. The complete event took nearly a week, during which the wave field was under a constant state of adjustment. Figures 2(a) and (b)

show the wind, significant wave height, barometric pressure, air, and sea temperatures from NOAA Buoy 42016 for 6½ days centered on the post-frontal time period.

The northeast region of the Gulf of Mexico can be characterized by seasonal wind fields: during the fall and winter, the winds are predominately northern; however, with northwest or southeast winds also occurring (FLORIDA A&M UNIVERSITY, 1988). The winter months (December to February) are marked by frequent frontal passages on time scales of less than one week (DIMEGO *et al.*, 1976; ROBERTS *et al.*, 1978; HENRY, 1979). Winds from the north to northeast are higher in magnitude than winds from other directions during this season in the northeast Gulf of Mexico (THOMPSON and LEMING, 1978; SCHROEDER and WISEMAN, 1985). KELLY (1991) reported during the fall and winter seasons 10-meter high wind speeds of ~10 m/sec; he used data from NOAA Buoy 42015, 5 km due north of NOAA Buoy 42016.

March can be considered a transition month between the winter and spring seasons, characterized by an increased percentage of southeast winds between fronts and a decrease in the number of fronts (DIMEGO *et al.*, 1976; HENRY, 1979; SCHROEDER and WISEMAN, 1985). The study area at the time of our observation was expected to have east to south winds, with periodic northerly winds as the result of frontal passages. Based upon this characteristic (*i.e.* large directional wind shifts), the previous selection of four directional quadrants (north, east, south, and west) was expected to provide insight in analyzing the directionality of the wave-energy. The meteorological naming convention was used for waves: a north wave moves from the north to the south. The quadrants were established for the total energy contained in bins 2 through 5 with the north quadrant containing wind-wave-energy with a mean wave direction from 315° to 045°. East, south, and west quadrants each contained the successive 90° sectors.

The general surface width of a cold front is on the order of 500 km. The typical speed of advance of this type of front is on the order of 10 to 15 m/sec. The passage of a cold front is marked by rapidly falling air temperature, rapidly rising barometric pressure, and veering (anticyclonic shift) in the wind field (WILLIAMS *et al.*, 1973; COLE, 1980; KOTSCH, 1983; HSU, 1988). The actual passage of a cold front does not occur instantaneously. It takes a finite period of time for the atmospheric parameters to shift from the pre-frontal values to the post-frontal values. This period of adjustment, from pre-frontal to post-front atmospheric conditions is expected to be on the order of 10 hours. Our front is typical in these regards as shown in Figure 2.

### FRONTAL PASSAGE PERIODS

The frontal passage event was partitioned into four periods: (1) prevailing seasonal conditions, (2) pre-frontal passage, (3) frontal passage, and (4) post-frontal passage. The partitioning of the periods was based upon the barometric pressure trends, the difference between the air and sea temperatures, and the hourly wind directions (Figure 2).

The prevailing seasonal conditions existed until March 8 at 1800 UTC (08/1800). The wind speed ( $U_5$ , the wind speed

at a height of 5 m) was fairly steady with a mean and standard deviation of  $2.6 \pm 0.6$  m/sec, and a direction of  $127^\circ \pm 19^\circ$ . The air temperature was approximately equal to the sea-surface temperature (SST); neutral atmospheric conditions were assumed to have existed. The surface barometric pressure was fairly steady. The significant wave height ( $H_s$ ) was approximately 0.5 m from the southwest to south direction. Based upon an assumed Rayleigh distribution to the wave heights, and using linear wave theory, the conversion between spectral wave-energy and  $H_s$  is (USACE, 1984):

$$H_s \sim 4 \cdot \left[ \int C11(f) df \right]^{0.5}. \quad (1)$$

Where the limits of integration were 0.0325 Hz to 0.485 Hz dictated by the buoy system used and  $C11(f)$  was centered on the frequency component  $f$ .

The pre-frontal passage period was from 08/1800 to 09/1800. Air temperature and SST remained fairly coupled, with air temperature slightly greater than SST. Surface pressure started to drop at a rate of approximately 1 hPa/hr to a low that occurred at the end of the period.  $U_5$  increased unsteadily from 4 to 10 m/sec. The wind direction was from the east-southeast. Significant wave height for this period was approximately 1 m.

The frontal passage period was from 09/1800 to 10/0100. The drop of surface pressure had stopped and showed a slight rise at the end of the period. Also at the end of the period, air temperature and SST were separated by ~1 °C, implying that the cold air behind the front had not yet reached NOAA Buoy 42016. The wind direction veered from the southeast to the southwest. The wind turbulence caused by the constantly changing wind speed tended to keep the lower air column well-mixed. The  $H_s$  had increased to a maximum of ~1.8 m.

The post-frontal period was from 10/0100 to 12/1200. Figure 1 shows the location of the front at 10/0300, several hours after the front had begun to pass the location of NOAA Buoy 42016. This period was marked by increasing surface pressure. Air temperature and SST had completely uncoupled; air temperature experienced a very sharp decrease to a minimum of ~6 °C, followed by a gradual rise to its pre-frontal value after several days. Sea surface temperature showed a slight decrease due to the presence of the cold air mass overlying the region. From 10/0600 until 11/1800 the average wind was northerly at  $8.4 \pm 1.9$  m/sec. This period also contained the peak wave-energy equivalent to a surface height variance of  $0.26 \text{ m}^2$  ( $H_s \sim 2.1$  m). After the occurrence of the peak wave-energy, wave-energy decayed to the prevailing seasonal condition level equivalent to ~0.05  $\text{m}^2$ .

Conditions returned to the pre-frontal seasonal conditions at ~12/1200. Air temperature and SST were nearly the same; neutral atmospheric conditions were returning.  $U_5$  remained steady at ~7 m/sec to 13/0000, after which it dropped to near 4 m/sec. The wind direction veered to the east, became weak and variable, and showed some possible sea-breeze components. During the veering period, the wave-energy increased from the low to a peak equivalent to  $0.10 \text{ m}^2$ , corresponding to an  $H_s$  of 1.26 m. The barometric pressure was higher, but dropped to the value prior to 08/1800.

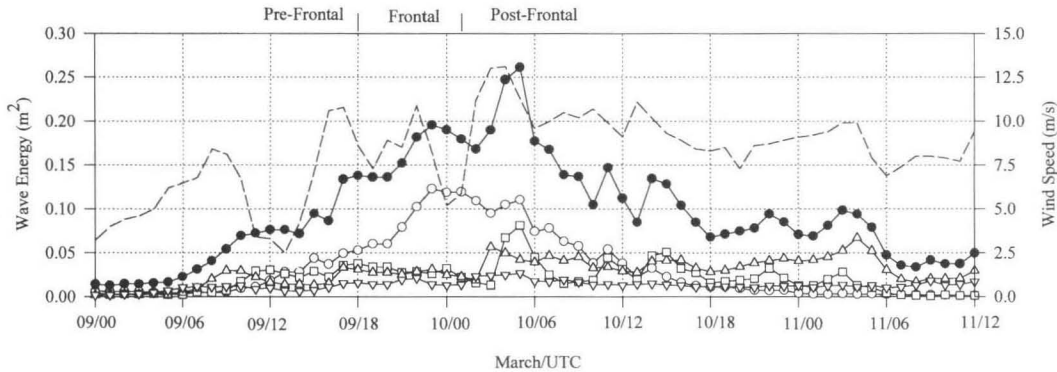


Figure 3. Time series of the binned frequency components of the wind and wave-energy field (not including the swell energy of bin 1). The data are based upon hourly spectral estimates from a 3-m discus buoy located at NOAA Buoy 42016. Bin 2 (○) contains wave-energy from 0.08 to 0.18 Hz, bin 3 (□) from 0.18 to 0.22 Hz, bin 4 (△) from 0.22 to 0.30 Hz, and bin 5 (▽) from 0.30 to 0.485 Hz. The total energy (●) contains the wind generated wave-energy from 0.08 to 0.485 Hz. The wind speed (---) is from the buoy anemometer located at a height of 5 m.

**DIRECTIONAL WAVE FIELDS**

During the pre-frontal passage period (08/1800 to 09/1800), the higher frequency bins responded to wind speed changes with less time lag in the uptake or transfer of the wind-wave-energy than lower frequency bins (Figure 3). At 09/0000, the wind was 3.2 m/sec at 130°; at 09/0800, the wind magnitude increased to a maximum of 8.4 m/sec, with a minor wind shift occurring of less than 30°. This was over a sixfold increase in wind-energy in eight hours. Wave-energy in bin 5 (frequencies greater than 0.30 Hz) increased at 09/0300, lagging the wind increase by three hours. Wave-energy in bin 4 (0.22 to 0.30 Hz) showed a sharp increase starting at 09/0600. Wave-energy in bin 3 (0.18 to 0.22 Hz) increased at 09/0900. The wave-energy in bin 2 (0.08 to 0.18 Hz) showed an increase at 09/1000. While the various frequency bins were responding to the initial wind-speed increase, at 09/0800 there was a substantial decrease in wind-energy, dropping from ~8 m/sec to ~3 m/sec in two hours. Winds were low in magnitude until 09/1300, wind speed then increased to a pre-frontal maximum, occurring at 09/1700. The lag between wind speed

changes and wave field responses for bins 2 through 5 were shorter than those noted for the first wind-speed increase.

During the frontal passage period (09/1800 to 10/0100), the seas were 100-percent southerly (Figure 4). This period contained the peak of the south wave-energy field, which occurred at 09/2300. The wave-energy was principally contained in the lowest wave-energy bin, bin 2. The sharp decrease in wind speed that occurred at 09/2200 did not result in a decrease in the wave-energy field until 10/0000.

The post-frontal period (10/0200 to 12/1200) was characterized by a steady, generally northerly wind direction, and a slowly decreasing wind speed. The wave field had two principal components: the old south wave field and the new north-west wave field. The new wave field energy was split between the north and west quadrants (Figure 4). The westerly wave field was the first to develop as the result of the wind field veering to a fairly steady north-northwest direction. The energy in the south quadrant initially decayed under the influence of the north-northwest wind field. At 10/0200 the majority of the wave-energy was still contained in the decaying

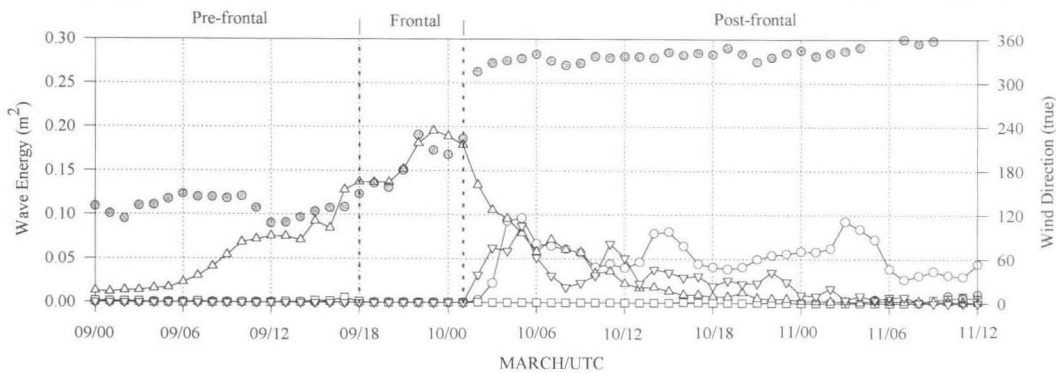


Figure 4. Time series of the directional wave-energy combined into four quadrants, each centered around the four cardinal points ○ North, □ East, △ South, and ▽ West). The data are based upon hourly spectral estimates from a 3-m discus buoy located at NOAA Buoy 42016. The wind direction (●) is from the buoy anemometer located at a height of 5 m.

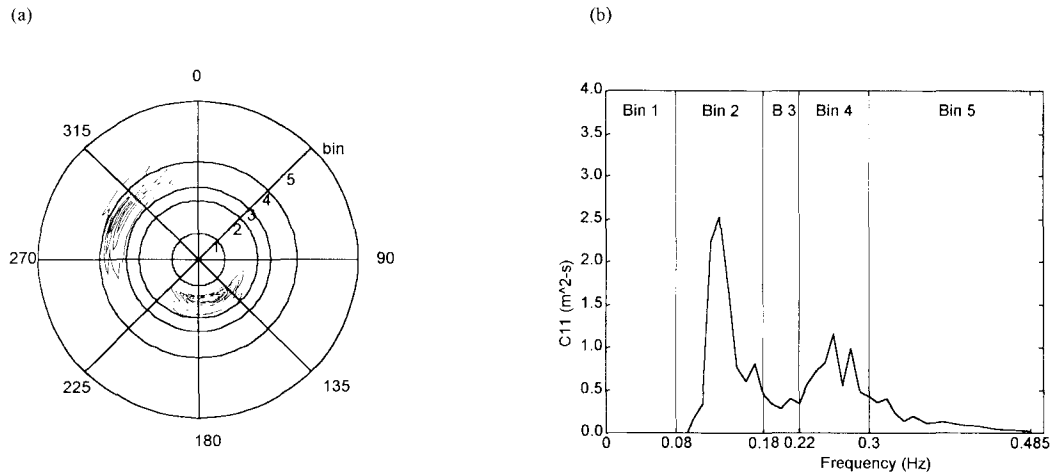


Figure 5. Hourly directional wave data for March 10, 1994, 0300 UTC. (a) Polar contour plot using 8 equally spaced contour intervals relative to this hour's peak energy. (b) Nondirectional heave spectra. Bin division is discussed within the text.

south quadrant wave field. However, at 10/0300 there was a reduction in the rate of decay of the south quadrant wave-energy. This was followed by an increase in the energy of the south quadrant wave field at 10/0700, while still under the influence of a north-northwest wind field. After 10/0700, the predominate direction of the wave field was from the north, with some energy contained in the western quadrant.

## DISCUSSION

There were two lag-time scales of interest in this study: (1) the time needed for energy to appear in a frequency region after an increase or decrease in the wind-energy level, and (2) the time needed for energy to decay in the old direction after a wind shift. The lag times that occurred after 09/0800 were considered representative for the time necessary for the uptake of energy from the wind field into the wave-energy field. Clearly, the choice of frequency boundaries for the energy bins biased the lag time for each bin; additional bins would have shown intermediate lag times. The energy in bin 5 was quickly transferred to other lower frequencies. The initial time lag for energy uptake was 3 hours for bin 5. This was followed by lags of 6, 9, and 10 hours for bins 4, 3, and 2, respectively. Though the wind magnitude fluctuated between 09/0800 and 09/1700, the magnitudes at 09/0700 and 09/1000 were nearly equal, as were they at 09/0800 and 09/0900. The sampling interval of one hour was the most restrictive agent in resolving and quantifying these time lag values.

GÜNTHER *et al.* (1981) examined the response of the wave field to changing wind directions using the JONSWAP model. They found that the momentum added by the new wind direction was transferred by nonlinear interactions to lower frequencies. The VAN VLEDDER and HOLTHUIJSEN (1988) model study using EXACT-NL showed that energy from the new wave field would be siphoned off into the old wave field, thereby slowing down the rate of decay of the old wave field. This enhancement of the old wave field by the new wave field

is documented in our data (Figure 4). The southerly wave field peaked at 09/2300, as soon as the winds shifted it became the "old" wave field. The old wave field decayed to a local minimum at 10/0600, but gained energy the next hour, followed by an unsteady decay until 11/1000. The time needed for the energy to decay or transit out of the region in the old direction was, thus, substantially altered.

The time series of the wind (Figure 2a) showed that during the frontal passage, the changes in both the magnitude and direction of the wind were not smooth in time. The conditions that existed during the frontal passage, especially during the post-frontal period, resulted in a very broad spectra in  $\theta$ -space, shown in the polar contour plots (Figures 5a-9a), and spectrally wide in  $f$ -space, shown in the heave spectra plots (Figures 5b-9b). During the pre-frontal and frontal periods, wind strength generally increased, but over the sampling periods of one hour fluctuations occurred. A single frequency band, as opposed to the frequency bins, would not have provided as insightful a picture of the time history of the wave-energy field, in terms of the lag response of the high-, mid-, and lower-frequency regions of the spectra. A single frequency would have shown a more rapid response to fluctuations in wind direction and speed; but this rapid response would mask out the general trend of the changes in wave-energy. The broader bin averaged out the rapid fluctuations and clearly showed the wave-energy trends. Additionally, bins have more degrees of freedom than the individual frequency bands, and the confidence limits around their values are improved. Further, the use of a "mid-range" frequency bin, instead of the highest frequency bin, as the wind-energy tracer, was supported by the energy bin time series (Figure 3). The gradual increase in wind-energy up to 09/0900 and the very rapid increase in wind-energy that occurred at 09/1300 and 10/0200 were accompanied by associated visible rises in bin 4. The rises in bin 5 were not sufficiently sustained to correlate well with the wind-speed changes. The wave-energy in bin 4 (0.22 to 0.30 Hz) provided the best wind-energy tracer

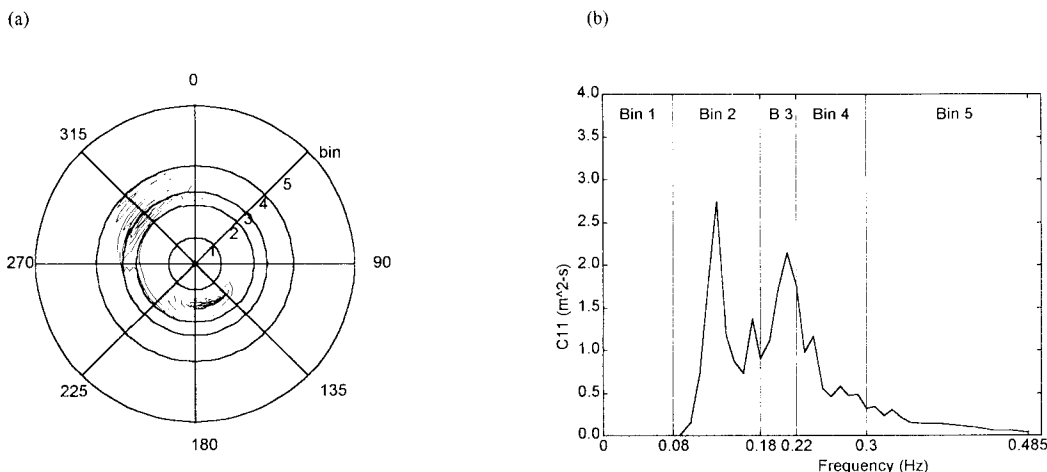


Figure 6. Hourly directional wave data for March 10, 1994, 0400 UTC. (a) Polar contour plot using 8 equally spaced contour intervals relative to this hour's peak energy. (b) Nondirectional heave spectra.

bin overall for use in understanding the hourly changes in the wave spectra. It followed increases and trends of wind-speed changes more closely than bin 5. The wave-energy in bin 5 rapidly attained saturation, and thus, its energy was dissipated down to bin 4.

Examination of binned wave-energy and directional time series (Figures 3 and 4), hourly directional wave contour and nondirectional energy spectra (*i.e.* heave) plots (Figures 5 through 9) provided evidence that energy was physically transferred from the north and west quadrants into the south quadrant. Between 10/0100 and 10/0300, the decay of the old south wave field was fairly steep. From 10/0300 to 10/0600, the rate of decay of this wave field was reduced. The decay rate changed signs (*i.e.* it became a rate of increasing energy) between 10/0600 and 10/0700. The north-northwest wind field was supporting a southerly wave field.

The energy increased in the new wave field after the wind shift at 10/0200, until the period of maximum wave-energy at 10/0500. During that period, wave-energy in bin 4 increased; the new wave field at 10/0300 was smaller than the old wave field (Figures 4 and 5). One hour later, the energy contained in bin 3 had increased, while the energy in bin 4 had decreased (Figures 3 and 6), implying a transfer to a lower frequency. The peak of the spectra in the old wave field energy (bin 2) remained centered at a fairly constant frequency (Figures 5 and 6). The new wave field was increasing in energy (Figure 4), with the energy moving towards lower frequencies (Figure 3). By 10/0500, the new wave field was larger than the old wave field (Figures 4 and 7). The old wave field remained more focused in its direction, *i.e.* narrower in  $\theta$ -space, than the new wave field from the northwest (Figures 5a, 6a, and 7a).

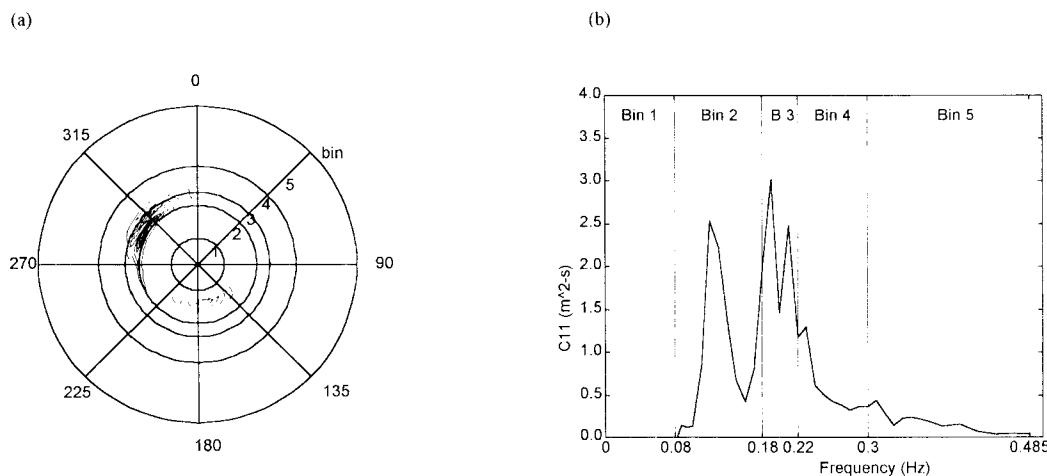


Figure 7. Hourly directional wave data for March 10, 1994, 0500 UTC. (a) Polar contour plot using 8 equally spaced contour intervals relative to this hour's peak energy. (b) Nondirectional heave spectra.

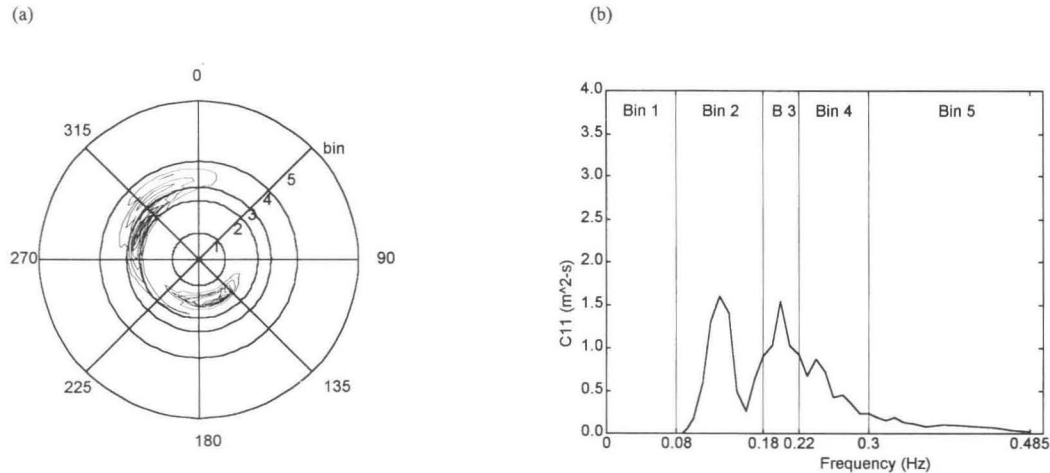


Figure 8. Hourly directional wave data for March 10, 1994, 0600 UTC. (a) Polar contour plot using 8 equally spaced contour intervals relative to this hour's peak energy. (b) Nondirectional heave spectra.

At 10/0600, the wave field was strongly bimodal (Figure 8). The values of the local spectral peaks for the old and new wave fields were distinct. At 10/0700, the heave spectra had dramatically changed (Figure 9b), the old wave field spectral peak increased by nearly a factor of two and had narrowed in  $f$ -space, while the new wave field spectral peak had decreased by a factor of two and moved back to a higher frequency. This increase of energy in the old wave field (southerly) and decrease in the new wave field (northwesterly) was done under the forcing of a fairly directionally stable north-northwest wind field (Figure 4).

The support of the southerly wave field appears not to have been continuous. The rate of decay of the south energy had two rate changes or "hinge" points (Figure 4), one at 10/0300 and the other at 10/0600. The polar contour plot for 10/0400 (Figure 6a) showed a narrow energy bridge connecting the old and new wave fields both in frequency and in direction. While at 10/0600 (Figure 8a), there was no connecting bridge as much as there was an overlap between the old and new wave fields directionally. The existence of overlaps or bridges corresponded well with the changes in the decay rate of the old south wave field and may provide a physical insight into the siphoning-off of energy discussed by VAN VLEDDER and HOLTHUIJSEN (1988). There was an increase in energy of the spectral peak at 10/0700, one hour after a spectral bridge existed. The correlation between the existence of an energy bridge and the enhancement of the southerly or old wave field supported the conclusions of VAN VLEDDER and HOLTHUIJSEN (1988), YOUNG *et al.* (1987), and QUANDUO and KOMEN (1993). That is, nonlinear wave-wave interactions tend to slow down the turning rate of the wave field.

It should be noted that the energy bridge was not an artifact of the cosine-2s directional energy spreading model. The energy bridge exists at frequencies determined by time series analysis of the buoy's acceleration. Its existence and correlation with a noticeable change in the rate of decay of the southern energy wave field support the assertion that the

energy bridge played a key role in the energy distribution of the wave field.

The wave data that was available for this study was the hourly transmitted NDBC data. As discussed previously, this represented a merging of 40-minute, 20-minute, and 10-minute sampling periods for the low-, mid-, and high-frequency portions of the wave spectrum. The discussed lag times and jumps in energy levels were likely actual wave field phenomenon. Clearly, though, there were processes that were taking place at periods of less than an hour.

## SUMMARY

Between 1800 UTC, March 8, 1994, and 1200 UTC, March 12, 1994 a cold front passage occurred in the northeast Gulf of Mexico containing a large direction and magnitude change in wind. The wave field's response to this event has been shown to contain some expected and unexpected results. One expected outcome was the shorter time lag between a change in the magnitude of the wind field and a corresponding change in the wave-energy field for higher frequency waves than for lower frequency waves. As projected by the work of VAN VLEDDER and HOLTHUIJSEN (1988) and YOUNG *et al.* (1987), under certain conditions a rapidly changing wind field direction and increase in wind speed can cause the formation of a new, directionally different, wave field. However, unexpectedly, there did exist some apparent exchange of energy between these two wave fields via a mid-range frequency energy bridge. The use of broader frequency bins vice typical frequency bands reduced the variability of the data and allowed this process to be identified.

Wave-wave interactions tend to resist directionally uncoupled energy fields as noted in the works of VAN VLEDDER and HOLTHUIJSEN (1988), YOUNG *et al.* (1987), and QUANDUO and KOMEN (1993). The two directionally different wave-energy fields existed during the post-frontal period as the result of  $\sim 135^\circ$  wind shift. Clearly shown with two polar contour

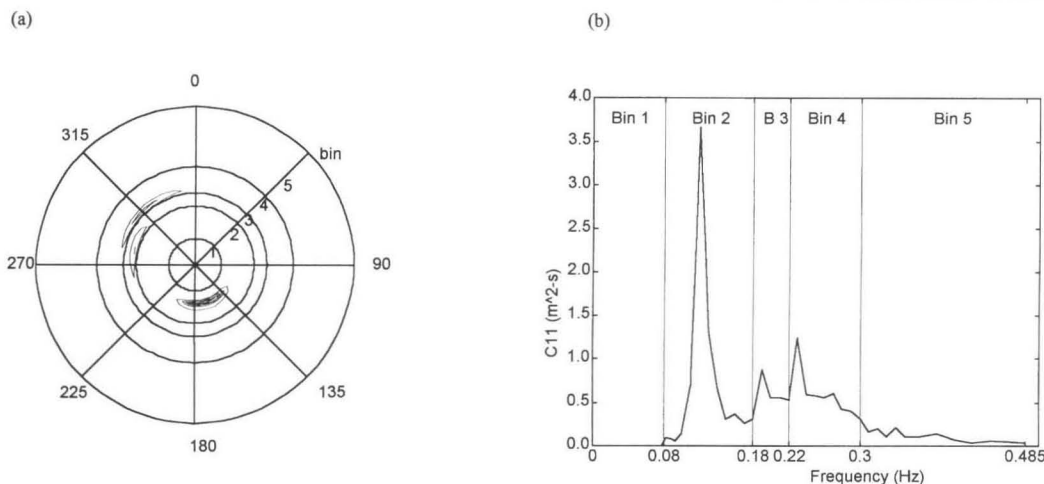


Figure 9. Hourly directional wave data for March 10, 1994, 0700 UTC. (a) Polar contour plot using 8 equally spaced contour intervals relative to this hour's peak energy. (b) Nondirectional heave spectra.

plots of directional wave spectra, a wave-energy bridge was created between the two fields. This bridging occurred either as a distinct (from the old and new wave fields) energy bridge or as an extension of a new wave field in  $\theta$ -space. This bridge formation was linked with an altered decay rate of the old wave field.

The technique used in establishing energy quadrants and mapping out a time series of their changes proved to be a valuable method for the analysis of directional wave fields. While heave spectra and polar contour plots of directional wave spectra provided insight for the finer details of the analysis, they did not provide as useful a tool as a time-series plot of the energies. The study region's seasonal wind field pattern was fortuitous in supporting the use of a simple four-quadrant system to examine the changes of the wave field energy in  $\theta$ -space. Other geographical settings may not allow such a simple system.

A quantitative analysis of the wind fields and the wave fields during a frontal passage will require a finer resolution in time. Future plans will focus on using available time-series records of buoy motion and wind data to examine this data set and others with wave spectra wind averages based upon multiple estimates per hour. Other techniques that allow bimodal energy spreading functions will be explored in analysis of wave-energy response to major wind shifts.

#### ACKNOWLEDGEMENTS

The work presented here was supported by the National Weather Service National Data Buoy Center, which provided the data used in this analysis, and the University of Southern Mississippi, Institute of Marine Sciences (previously the Center for Marine Science). We wish to thank Mr. D. Henderson, Mr. K. Steele, Dr. C.-C. Teng, and Dr. D. Wang for their support and assistance in the collection and discussion of the data used. Additionally, the two journal reviewers Dr. S. Dimarco and Dr. G. Stone provided constructive reviews of this manuscript.

#### LITERATURE CITED

- ACINAS, J.R., 1988. A directional prediction model of waves and variable wind. *Coastal Engineering*, 698-703.
- ALLENDER, J.H.; ALBRECHT, J., and HAMILTON, G.D., 1983. Observations of directional relaxation of wind sea spectra. *Journal of Physical Oceanography*, 13, 1519-1525.
- COLE, F.W., 1980. *Introduction to Meteorology*. New York: Wiley, 505p.
- DIMEGO, G.J.; BOSART, L.F., and ENDERSEN, W.W., 1976. An Examination of the frequency and mean conditions surrounding frontal incursions into the Gulf of Mexico and Caribbean Sea. *Monthly Weather Review*, 104, 709-718.
- EARLE, M.D., 1994. National Data Buoy Center non-directional and directional wave data analysis procedures. *NDBC/CSC Technical Report CSC/ATD-91-C-002*, 66p.
- FLORIDA A&M UNIVERSITY, 1988. *Meteorological Database and Synthesis for the Gulf of Mexico*. OCS Study/MMS 88-0064. U.S. Department of the Interior, Minerals Mgmt. Service, Gulf of Mexico OCS Regional Office, New Orleans, LA, 486p.
- GUNTHER, H.; ROSENTHAL, W., and DUNCKEL, M., 1981. The response of surface gravity waves to changing wind direction. *Journal of Physical Oceanography*, 11, 718-728.
- HENRY, W.K., 1979. Some aspects of the fate of cold fronts in the Gulf of Mexico. *Monthly Weather Review*, 107, 1078-1082.
- HSU, S.A., 1988. *Coastal Meteorology*, San Diego: Academic, 237p.
- JACKSON, F.C. and JENSEN, R.E., 1995. Wave field response to frontal passages during SWADE. *Journal of Coastal Research*, 11, 34-67.
- KELLY, F.J., 1991. Physical oceanography/water mass characterization. In: BROOKS, J.M. (ed.), *Mississippi-Alabama Continental Shelf Ecosystem Study. Data Summation and Synthesis, Volume II, Technical Narrative*. OCS Study MMS-91-0063, U.S. Department of the Interior, Minerals Management Service, Gulf of Mexico OCS Region Office, New Orleans, Louisiana, Chap 10.
- KOTSCH, W.J., 1983. *Weather for the Mariner*. Annapolis, Maryland: Naval Institute Press, 253p.
- LONGUET-HIGGINS, M.S.; CARTWRIGHT, D.E., and SMITH, N.D., 1963. Observations of the directional spectrum of sea waves using the motions of a floating buoy. *Ocean Wave Spectra*. Englewood Cliffs, New Jersey: Prentice-Hall.
- MASSON, D., 1990. Observations of the response of sea waves to veering winds. *Journal of Physical Oceanography*, 20, 1876-1885.
- QUANDUO, G. and KOMEN, G., 1993. Directional response of ocean

- waves to changing wind direction. *Journal of Physical Oceanography*, 23, 1561–1566.
- ROBERTS, H.H.; HUI, O.K.; HSU, S.A.; ROUSE, L.J., JR., and RICKMAN, D., 1987. Impact of cold-front passages on geomorphic evolution and sediment dynamics of the complex Louisiana coast. *Coastal Sediments '87, II* (ASCE Conference, May 12–14, 1987, New Orleans, Louisiana), pp. 1950–1963.
- SCHROEDER, W.W. and WISEMAN, W.J., JR., 1985. An analysis of the winds (1974–1984) and sea level elevation (1973–1983) in coastal Alabama. *Mississippi-Alabama Sea Grant Consortium, MASGP-84-024*, 102p.
- STEELE, K.E.; LAU, J.C.-C., and HSU, Y.-H.L., 1985. Theory and application of calibration techniques for an NDBC directional wave measurement buoy. *IEEE Journal of Oceanic Engineering*, OE-10(4), 382–396.
- STEELE, K.E.; TENG, C.-C., and WANG, D.W.C., 1992. Wave Direction Measurements Using Pitch-Roll Buoys. *Ocean Engineering*, 19(4), 349–375.
- THOMPSON, P.A. and LEMING, T.D., 1978. Seasonal description of winds and surface and bottom salinities and temperatures in the northern Gulf of Mexico, October 1972 to January 1976. *NOAA Technical Report, NMFS SSRT-719*.
- TUCKER, M.J., 1989. Interpreting directional data from large pitch-roll-heave buoys. *Ocean Engineering*, 16, 173–192.
- U.S. ARMY CORPS OF ENGINEERS (USACE), 1984. *Shore Protection Manual*. Vicksburg, Mississippi: USACE, Waterways Experiment Station, Corps of Engineers Coastal Engineering Research Center.
- VAN VLEDDER, G.P. and HOLTHUIJSEN, L.H., 1988. Waves in turning wind fields. *21st Coastal Engineering Conference* (June 20–25, 1988, Coasta Del Sol-Malaga Spain), pp. 602–611.
- VAN VLEDDER, G.P. and HOLTHUIJSEN, L.H., 1993. The directional response of ocean waves to turning winds. *Journal of Physical Oceanography*, 23, 177–192.
- WANG, D.W.-C.; TENG, C.-C., and STEELE, K.E., 1989. Buoy directional wave observations in high seas. *Marine Technical Society OCEANS 1989 Proceedings*, pp. 1416–1420.
- WILLIAMS, J.; HIGGINSON, J.J., and ROHRBOUGH, J.D., 1973. *Sea & Air The Marine Environment*. Annapolis, Maryland: Naval Institute Press.
- YOUNG, I.R., 1994. On the measurement of directional wave spectra. *Applied Ocean Research* 16, 283–294.
- YOUNG, I.R.; HASSELMANN, S., and HASSELMANN, K., 1987. Computations of the response of a wave spectrum to a sudden change in wind direction. *Journal of Physical Oceanography*, 17, 1317–1337.